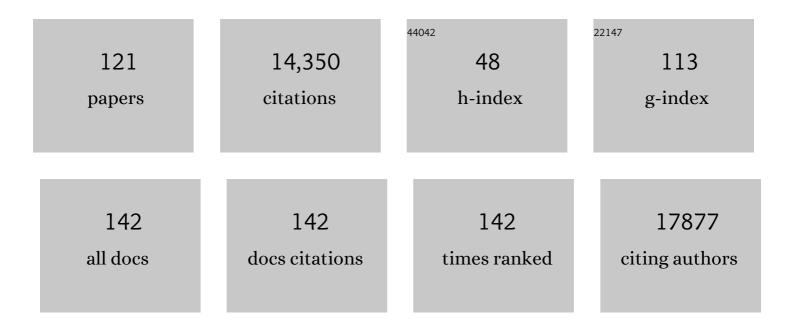
## Osamu Nureki

List of Publications by Year in descending order

Source: https://exaly.com/author-pdf/8049336/publications.pdf Version: 2024-02-01



#	Article	IF	CITATIONS
1	Genome-scale transcriptional activation by an engineered CRISPR-Cas9 complex. Nature, 2015, 517, 583-588.	13.7	2,272
2	Crystal Structure of Cas9 in Complex with Guide RNA and Target DNA. Cell, 2014, 156, 935-949.	13.5	1,690
3	Engineered CRISPR-Cas9 nuclease with expanded targeting space. Science, 2018, 361, 1259-1262.	6.0	783
4	Crystal Structure of Cpf1 in Complex with Guide RNA and Target DNA. Cell, 2016, 165, 949-962.	13.5	552
5	Somatic RHOA mutation in angioimmunoblastic T cell lymphoma. Nature Genetics, 2014, 46, 171-175.	9.4	542
6	Light-induced structural changes and the site of O=O bond formation in PSII caught by XFEL. Nature, 2017, 543, 131-135.	13.7	515
7	Crystal structure of the channelrhodopsin light-gated cation channel. Nature, 2012, 482, 369-374.	13.7	503
8	Crystal Structure of Staphylococcus aureus Cas9. Cell, 2015, 162, 1113-1126.	13.5	357
9	Engineered Cpf1 variants with altered PAM specificities. Nature Biotechnology, 2017, 35, 789-792.	9.4	351
10	A three-dimensional movie of structural changes in bacteriorhodopsin. Science, 2016, 354, 1552-1557.	6.0	350
11	Structural basis for recognition of the tra mRNA precursor by the Sex-lethal protein. Nature, 1999, 398, 579-585.	13.7	349
12	Structure and Engineering of Francisella novicida Cas9. Cell, 2016, 164, 950-961.	13.5	296
13	Cap-specific terminal <i>N</i> <sup>6</sup> -methylation of RNA by an RNA polymerase II–associated methyltransferase. Science, 2019, 363, .	6.0	262
14	Structural basis for Na+ transport mechanism by a light-driven Na+ pump. Nature, 2015, 521, 48-53.	13.7	224
15	Structural Basis for the Canonical and Non-canonical PAM Recognition by CRISPR-Cpf1. Molecular Cell, 2017, 67, 633-645.e3.	4.5	206
16	Structural basis for dynamic mechanism of proton-coupled symport by the peptide transporter POT. Proceedings of the National Academy of Sciences of the United States of America, 2013, 110, 11343-11348.	3.3	197
17	Real-space and real-time dynamics of CRISPR-Cas9 visualized by high-speed atomic force microscopy. Nature Communications, 2017, 8, 1430.	5.8	184
18	Recurrent somatic mutations underlie corticotropin-independent Cushing's syndrome. Science, 2014, 344, 917-920.	6.0	177

#	Article	IF	CITATIONS
19	Crystal structure of the MgtE Mg2+ transporter. Nature, 2007, 448, 1072-1075.	13.7	166
20	Activation mechanism of endothelin ETB receptor by endothelin-1. Nature, 2016, 537, 363-368.	13.7	148
21	Crystal Structure of the Minimal Cas9 from Campylobacter jejuni Reveals the Molecular Diversity in the CRISPR-Cas9 Systems. Molecular Cell, 2017, 65, 1109-1121.e3.	4.5	145
22	Cryo-EM structures capture the transport cycle of the P4-ATPase flippase. Science, 2019, 365, 1149-1155.	6.0	143
23	Base editors for simultaneous introduction of C-to-T and A-to-G mutations. Nature Biotechnology, 2020, 38, 865-869.	9.4	137
24	An enzyme with a deep trefoil knot for the active-site architecture. Acta Crystallographica Section D: Biological Crystallography, 2002, 58, 1129-1137.	2.5	122
25	Amplification-free RNA detection with CRISPR–Cas13. Communications Biology, 2021, 4, 476.	2.0	119
26	Crystal Structure of Silkworm PIWI-Clade Argonaute Siwi Bound to piRNA. Cell, 2016, 167, 484-497.e9.	13.5	116
27	Crystal structure of Enpp1, an extracellular glycoprotein involved in bone mineralization and insulin signaling. Proceedings of the National Academy of Sciences of the United States of America, 2012, 109, 16876-16881.	3.3	114
28	Structural insights into tetraspanin CD9 function. Nature Communications, 2020, 11, 1606.	5.8	114
29	Crystal structure of the red light-activated channelrhodopsin Chrimson. Nature Communications, 2018, 9, 3949.	5.8	112
30	Cryo-EM structure of the human L-type amino acid transporter 1 in complex with glycoprotein CD98hc. Nature Structural and Molecular Biology, 2019, 26, 510-517.	3.6	110
31	Structural insights into cGAMP degradation by Ecto-nucleotide pyrophosphatase phosphodiesterase 1. Nature Communications, 2018, 9, 4424.	5.8	108
32	Cryo-EM structures of the human volume-regulated anion channel LRRC8. Nature Structural and Molecular Biology, 2018, 25, 797-804.	3.6	104
33	Outward- and inward-facing structures of a putative bacterial transition-metal transporter with homology to ferroportin. Nature Communications, 2015, 6, 8545.	5.8	103
34	Structural insights into ligand recognition by the lysophosphatidic acid receptor LPA6. Nature, 2017, 548, 356-360.	13.7	101
35	Structure of the miniature type V-F CRISPR-Cas effector enzyme. Molecular Cell, 2021, 81, 558-570.e3.	4.5	95
36	Mg2+-dependent gating of bacterial MgtE channel underlies Mg2+ homeostasis. EMBO Journal, 2009, 28, 3602-3612.	3.5	94

3

#	Article	IF	CITATIONS
37	Structural Basis for Potent Inhibition of SIRT2 Deacetylase by a Macrocyclic Peptide Inducing Dynamic Structural Change. Structure, 2014, 22, 345-352.	1.6	79
38	X-ray structures of endothelin ETB receptor bound to clinical antagonist bosentan and its analog. Nature Structural and Molecular Biology, 2017, 24, 758-764.	3.6	79
39	Atomistic design of microbial opsin-based blue-shifted optogenetics tools. Nature Communications, 2015, 6, 7177.	5.8	78
40	Data processing pipeline for serial femtosecond crystallography at SACLA. Journal of Applied Crystallography, 2016, 49, 1035-1041.	1.9	76
41	Capturing an initial intermediate during the P450nor enzymatic reaction using time-resolved XFEL crystallography and caged-substrate. Nature Communications, 2017, 8, 1585.	5.8	74
42	Structural Basis for the Counter-Transport Mechanism of a H <sup>+</sup> /Ca <sup>2+</sup> Exchanger. Science, 2013, 341, 168-172.	6.0	73
43	Structural basis for channel conduction in the pump-like channelrhodopsin ChRmine. Cell, 2022, 185, 672-689.e23.	13.5	72
44	Crystal structure of heliorhodopsin. Nature, 2019, 574, 132-136.	13.7	71
45	Taste transduction and channel synapses in taste buds. Pflugers Archiv European Journal of Physiology, 2021, 473, 3-13.	1.3	70
46	<scp>ENPP</scp> 1 processes protein <scp>ADP</scp> â€ribosylation <i>in vitro</i> . FEBS Journal, 2016, 283, 3371-3388.	2.2	63
47	Structural basis for amino acid export by DMT superfamily transporter YddG. Nature, 2016, 534, 417-420.	13.7	60
48	Crystal structures of human ETB receptor provide mechanistic insight into receptor activation and partial activation. Nature Communications, 2018, 9, 4711.	5.8	60
49	Water-Containing Hydrogen-Bonding Network in the Active Center of Channelrhodopsin. Journal of the American Chemical Society, 2014, 136, 3475-3482.	6.6	59
50	Structural and functional insights into IZUMO1 recognition by JUNO in mammalian fertilization. Nature Communications, 2016, 7, 12198.	5.8	58
51	Structure of the triose-phosphate/phosphate translocator reveals the basis of substrate specificity. Nature Plants, 2017, 3, 825-832.	4.7	51
52	Crystal structure of plant vacuolar iron transporter VIT1. Nature Plants, 2019, 5, 308-315.	4.7	51
53	The structure of lipid nanodisc-reconstituted TRPV3 reveals the gating mechanism. Nature Structural and Molecular Biology, 2020, 27, 645-652.	3.6	51
54	Transport Cycle of Plasma Membrane Flippase ATP11C by Cryo-EM. Cell Reports, 2020, 32, 108208.	2.9	50

#	Article	IF	CITATIONS
55	Structural and Functional Analysis of DDX41: a bispecific immune receptor for DNA and cyclic dinucleotide. Scientific Reports, 2016, 6, 34756.	1.6	43
56	Crystal structure of Drosophila Piwi. Nature Communications, 2020, 11, 858.	5.8	42
57	Structural basis for ion selectivity revealed by high-resolution crystal structure of Mg2+ channel MgtE. Nature Communications, 2014, 5, 5374.	5.8	41
58	Time-resolved serial femtosecond crystallography reveals early structural changes in channelrhodopsin. ELife, 2021, 10, .	2.8	41
59	Realâ€ŧime observation of flexible domain movements in CRISPR–Cas9. EMBO Journal, 2018, 37, .	3.5	39
60	Cryo-EM structure of the human PAC1 receptor coupled to an engineered heterotrimeric G protein. Nature Structural and Molecular Biology, 2020, 27, 274-280.	3.6	39
61	DUSP10 constrains innate IL-33-mediated cytokine production in ST2hi memory-type pathogenic Th2 cells. Nature Communications, 2018, 9, 4231.	5.8	35
62	Cryo-EM structure of the volume-regulated anion channel LRRC8D isoform identifies features important for substrate permeation. Communications Biology, 2020, 3, 240.	2.0	35
63	Structural basis of gating modulation of Kv4 channel complexes. Nature, 2021, 599, 158-164.	13.7	35
64	Resonance Raman Investigation of the Chromophore Structure of Heliorhodopsins. Journal of Physical Chemistry Letters, 2018, 9, 6431-6436.	2.1	33
65	Crystal structure of human endothelin ETB receptor in complex with peptide inverse agonist IRL2500. Communications Biology, 2019, 2, 236.	2.0	33
66	Structural basis for the promiscuous PAM recognition by Corynebacterium diphtheriae Cas9. Nature Communications, 2019, 10, 1968.	5.8	33
67	The Catalytic Domain of Topological Knot tRNA Methyltransferase (TrmH) Discriminates between Substrate tRNA and Nonsubstrate tRNA via an Induced-fit Process. Journal of Biological Chemistry, 2013, 288, 25562-25574.	1.6	32
68	Cryo-EM structures of calcium homeostasis modulator channels in diverse oligomeric assemblies. Science Advances, 2020, 6, eaba8105.	4.7	32
69	Chimeras of Channelrhodopsin-1 and -2 from Chlamydomonas reinhardtii Exhibit Distinctive Light-induced Structural Changes from Channelrhodopsin-2. Journal of Biological Chemistry, 2015, 290, 11623-11634.	1.6	31
70	Cryo-EM structure of the human MT1–Gi signaling complex. Nature Structural and Molecular Biology, 2021, 28, 694-701.	3.6	31
71	Structural insights into the mechanism of rhodopsin phosphodiesterase. Nature Communications, 2020, 11, 5605.	5.8	30
72	Automated amplification-free digital RNA detection platform for rapid and sensitive SARS-CoV-2 diagnosis. Communications Biology, 2022, 5, .	2.0	28

#	Article	IF	CITATIONS
73	Crystal structure of schizorhodopsin reveals mechanism of inward proton pumping. Proceedings of the United States of America, 2021, 118, .	3.3	26
74	Ultrafast Dynamics of Heliorhodopsins. Journal of Physical Chemistry B, 2019, 123, 2507-2512.	1.2	24
75	Structural basis of the regulation of the normal and oncogenic methylation of nucleosomal histone H3 Lys36 by NSD2. Nature Communications, 2021, 12, 6605.	5.8	23
76	Glutamyl-tRNA synthetase from Thermus thermophilus HB8. Molecular cloning of the gltX gene and crystallization of the overproduced protein. FEBS Journal, 1992, 204, 465-472.	0.2	22
77	Spectroscopic study of the transmembrane domain of a rhodopsin–phosphodiesterase fusion protein from a unicellular eukaryote. Journal of Biological Chemistry, 2019, 294, 3432-3443.	1.6	22
78	Cryo-EM reveals mechanistic insights into lipid-facilitated polyamine export by human ATP13A2. Molecular Cell, 2021, 81, 4799-4809.e5.	4.5	22
79	Cryo-EM structure of the β3-adrenergic receptor reveals the molecular basis of subtype selectivity. Molecular Cell, 2021, 81, 3205-3215.e5.	4.5	21
80	Structure of the Dicer-2–R2D2 heterodimer bound to a small RNA duplex. Nature, 2022, 607, 393-398.	13.7	20
81	Consensus mutagenesis approach improves the thermal stability of system x <sub>c</sub> <sup>â^`</sup> transporter, <scp>xCT</scp> , and enables <scp>cryoâ€EM</scp> analyses. Protein Science, 2020, 29, 2398-2407.	3.1	19
82	Crystal structure of human endothelin ETB receptor in complex with sarafotoxin S6b. Biochemical and Biophysical Research Communications, 2020, 528, 383-388.	1.0	19
83	Engineered Campylobacter jejuni Cas9 variant with enhanced activity and broader targeting range. Communications Biology, 2022, 5, 211.	2.0	19
84	The identity determinants required for the discrimination between tRNAGlu and tRNAAsp by glutamyl-tRNA synthetase from Escherichia coli. FEBS Journal, 1999, 261, 354-360.	0.2	18
85	Free Energy Landscape for the Entire Transport Cycle of Triose-Phosphate/Phosphate Translocator. Structure, 2018, 26, 1284-1296.e4.	1.6	17
86	Expression, purification, crystallization and preliminary X-ray crystallographic analysis of Enpp1. Acta Crystallographica Section F: Structural Biology Communications, 2012, 68, 778-782.	0.7	16
87	Mechanisms for Two-Step Proton Transfer Reactions in the Outward-Facing Form of MATE Transporter. Biophysical Journal, 2016, 110, 1346-1354.	0.2	16
88	An Atomistic Model of a Precursor State of Light-Induced Channel Opening of Channelrhodopsin. Biophysical Journal, 2018, 115, 1281-1291.	0.2	15
89	Structure of the human secretin receptor coupled to an engineered heterotrimeric G protein. Biochemical and Biophysical Research Communications, 2020, 533, 861-866.	1.0	15
90	Structural basis for unique color tuning mechanism in heliorhodopsin. Biochemical and Biophysical Research Communications, 2020, 533, 262-267.	1.0	14

#	Article	IF	CITATIONS
91	Crystallization of the human tetraspanin protein CD9. Acta Crystallographica Section F, Structural Biology Communications, 2019, 75, 254-259.	0.4	14
92	Recognition of the Anticodon Loop of tRNA <sup>lle</sup> <sub>1</sub> by Isoleucyl-tRNA Synthetase from <i>Escherichia coli</i> . Nucleosides & Nucleotides, 1994, 13, 1231-1237.	0.5	13
93	Crystal structure of Cex1p reveals the mechanism of tRNA trafficking between nucleus and cytoplasm. Nucleic Acids Research, 2013, 41, 3901-3914.	6.5	13
94	t <scp>RNA</scp> â€dependent alanylation of diacylglycerol and phosphatidylglycerol in <scp><i>C</i></scp> <i>orynebacterium glutamicum</i> . Molecular Microbiology, 2015, 98, 681-693.	1.2	13
95	Crystal structure of Saccharomyces cerevisiae mitochondrial GatFAB reveals a novel subunit assembly in tRNA-dependent amidotransferases. Nucleic Acids Research, 2014, 42, 6052-6063.	6.5	12
96	Structure of the type V-C CRISPR-Cas effector enzyme. Molecular Cell, 2022, 82, 1865-1877.e4.	4.5	12
97	A three-dimensional structure model of the complex of glutamyl-tRNA synthetase and its cognate tRNA. FEBS Letters, 1995, 377, 77-81.	1.3	11
98	Peripheral tolerance by Treg via constraining OX40 signal in autoreactive T cells against desmoglein 3, a target antigen in pemphigus. Proceedings of the National Academy of Sciences of the United States of America, 2021, 118, e2026763118.	3.3	11
99	Conformational alterations in unidirectional ion transport of a light-driven chloride pump revealed using X-ray free electron lasers. Proceedings of the National Academy of Sciences of the United States of America, 2022, 119, .	3.3	11
100	Functional roles of Mg2+ binding sites in ion-dependent gating of a Mg2+ channel, MgtE, revealed by solution NMR. ELife, 2018, 7, .	2.8	10
101	Structural basis for oligomerization of the prokaryotic peptide transporter PepT <sub>So2</sub> . Acta Crystallographica Section F, Structural Biology Communications, 2019, 75, 348-358.	0.4	10
102	Crystallization and preliminary X-ray diffraction analysis of the full-length Mg <sup>2+</sup> transporter MgtE. Acta Crystallographica Section F: Structural Biology Communications, 2007, 63, 682-684.	0.7	9
103	Cryo-EM structures of the $\hat{1}^23$ adrenergic receptor bound to solabegron and isoproterenol. Biochemical and Biophysical Research Communications, 2022, 611, 158-164.	1.0	9
104	Recent Advances in the Structural Biology of the Volume-Regulated Anion Channel LRRC8. Frontiers in Pharmacology, 2022, 13, .	1.6	8
105	The mechanism of protein export enhancement by the SecDF membrane component. Biophysics (Nagoya-shi, Japan), 2011, 7, 129-133.	0.4	7
106	Crystal structure of channelrhodopsin, a light-gated cation channel - all cations lead through the monomer Biophysics (Nagoya-shi, Japan), 2013, 9, 57-61.	0.4	7
107	Cell-Free Synthesis of Human Endothelin Receptors and Its Application to Ribosome Display. Analytical Chemistry, 2022, 94, 3831-3839.	3.2	6
108	Spatial distribution of cytoplasmic domains of the Mg2+-transporter MgtE, in a solution lacking Mg2+, revealed by paramagnetic relaxation enhancement. Biochimica Et Biophysica Acta - Proteins and Proteomics, 2012, 1824, 1129-1135.	1.1	5

#	Article	IF	CITATIONS
109	Recent structural studies on Dom34/aPelota and Hbs1/aEF1α: important factors for solving general problems of ribosomal stall in translation. Biophysics (Nagoya-shi, Japan), 2013, 9, 131-140.	0.4	5
110	Vibrational and Molecular Properties of Mg <sup>2+</sup> Binding and Ion Selectivity in the Magnesium Channel MgtE. Journal of Physical Chemistry B, 2018, 122, 9681-9696.	1.2	5
111	Cryo-EM structures of thylakoid-located voltage-dependent chloride channel VCCN1. Nature Communications, 2022, 13, 2505.	5.8	5
112	Is zucchini a phosphodiesterase or a ribonuclease?. Biomedical Journal, 2014, 37, 369.	1.4	3
113	Lateral access mechanism of LPA receptor probed by molecular dynamics simulation. PLoS ONE, 2022, 17, e0263296.	1.1	3
114	Somatic G17V Rhoa Mutation Specifies Angioimmunoblastic T-Cell Lymphoma. Blood, 2013, 122, 815-815.	0.6	2
115	Structural Basis for Dynamic Mechanism of Proton-Coupled Symport by the Peptide Transporter POT. Seibutsu Butsuri, 2014, 54, 085-090.	0.0	1
116	Cex1 is a component of the COPI intracellular trafficking machinery. Biology Open, 2021, 10, .	0.6	0
117	Structural Basis for mRNA Surveillance by Archaeal Pelota and GTP-bound EF1α Complex. Seibutsu Butsuri, 2012, 52, 182-185.	0.0	0
118	Crystal Structure of Channelrhodopsin, a Light-Gated Cation Channel. Seibutsu Butsuri, 2013, 53, 246-249.	0.0	0
119	Aminoacyl-tRNA Synthetase : Structural Basis for the Substrate Recognition and the Molecular Evolution. Nihon Kessho Gakkaishi, 1996, 38, 60-67.	0.0	0
120	Structural Basis for the Molecular Evolution of Glutamyl-tRNA Synthetase Seibutsu Butsuri, 1997, 37, 321-325.	0.0	0
121	Cryo-EM Structure of the β3 Adrenergic Receptor Reveals the Molecular Basis of Subtype Selectivity. SSRN Electronic Journal, 0, , .	0.4	0